A Compact and Broadband Photonic Crystal Fiber Polarization Filter Based on a Plasmonic Resonant Thin Gold Film

Min Chang
Baixuan Li
Nan Chen
Xinglian Lu
Xuedian Zhang
Jian Xu
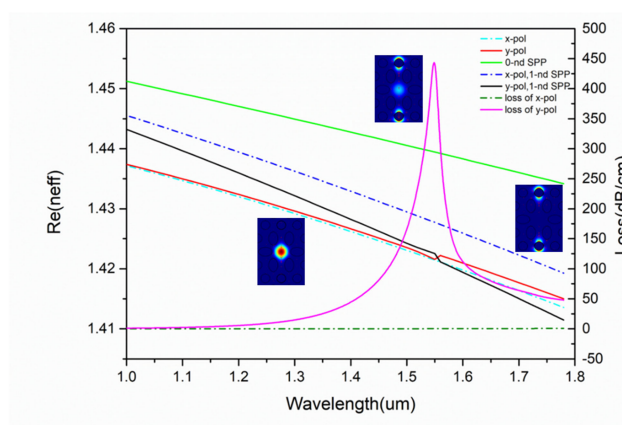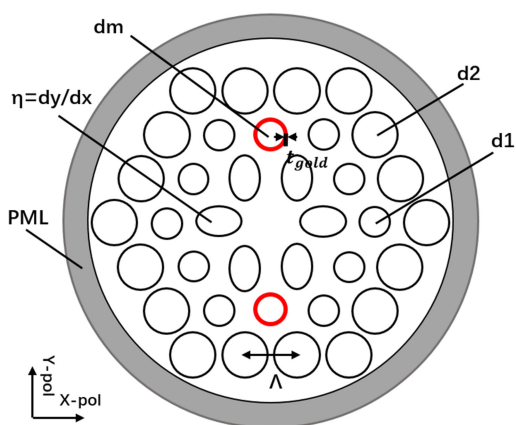
IEEE

A Compact and Broadband Photonic Crystal Fiber Polarization Filter Based on a Plasmonic Resonant Thin Gold Film

Min Chang [iD],[1] Baixuan Li,[1] Nan Chen,[1] Xinglian Lu [iD],[1] Xuedian Zhang,[1] and Jian Xu[2]

[1]Shanghai Key Laboratory of Modern Optical System, School of Optical-Electrical and Computer Engineering, University of Shanghai for Science and Technology, Shanghai 200093, China
[2]Department of Engineering Science and Mechanics, The Pennsylvania State University, University Park, PA 16802 USA

Abstract: A novel high birefringence gold-coated photonic crystal fiber (PCF) polarization filter based on surface plasmon resonance is proposed. The six elliptical holes arranged in a specific mode surrounding the core are utilized to gain high birefringence, and gold is coated inside the air holes to generate surface plasmons. By improving structural parameters, we achieve one state of polarization to propagate through the filter whereas the other state is severely attenuated. Specially, in the 1550 nm communication band, the confinement loss of *y*-polarized mode can reach 442 dB/cm while the corresponding loss of *x*-polarized mode is only 0.0316 dB/cm. The distinction between two losses is more than 10 000 times. In addition, when the length of the designed PCF filter is 1 mm, an extinction ratio of 326 dB/cm is obtained. The applicable bandwidth is up to 300 nm while the fiber length is merely 50 μm, which is better than other reported literatures. Owing to above-mentioned characteristics, the proposed polarization filter can be widely applied in compact and broadband filters in the communication band.

Index Terms: Photonic crystal fiber, surface plasmons, polarization filter.

1. Introduction

As a new type of fiber structure, photonic crystal fibers (PCFs) have a flexible design with the unique periodic arrangement of air holes. The researches show that PCFs have a series of diverse optical properties [1]–[4]. In recent years, with the development of materials science, some researchers have creatively combined new materials with PCFs, such as filling liquid crystals or magnetic fluids in the holes and coating graphene or metals on the inner wall of the holes [5]–[8]. Exploring application value from both theoretical and practical aspects, photonic crystal devices can not only replace traditional electronic devices, but also play important roles in optical communications, imaging, and biosensors [9]–[11]. Optical filters are applied widely in optical communication systems. The bulky size of traditional polarization filters has been unable to adapt to the development of optical communication technologies. It is imperative to find new devices with small size, wide bandwidth and good filter performance [12]–[14].

Surface plasmon resonance (SPR) can be effectively applied to new PCF polarization filters [15], [16]. As we all know, the free electrons moving on the metal surface can be regarded as a surface plasmon. When the frequency of the electromagnetic wave is equal to the frequency of the plasma oscillation, resonance will occur. Therefore, a resonance peak appears in the absorption spectrum. Recently, an increase number of researchers focus on this field. In 2011, Akira Nagasaki obtained high polarization transmission characteristics in PCF by introducing several metal wires closely arranged in the cladding [17]. In 2015, A. Khaleque and H. T. Hattori proposed broadband and compact polarization splitter which is capable of working in the infrared and mid-infrared wavelength ranges [18]. In 2017, Linghong Jiang and Yi Zheng numerically simulated a single polarization filter. In the 1.25–2.1 um wavelength range, the loss of the x polarization core mode is better than 248.95 dB/cm, while the loss of y polarization core mode is less than 0.21 dB/cm [19]. Polarization filters applied to the communication band, especially at 1550 nm, have many advantages. It is worth nothing that the light wave with a wavelength of 1550 nm has the least attenuation loss when propagating in the fiber, which can meet the long-distance propagation.

In this paper, a birefringence and broadband single-channel PCF polarization filter based on SPR with a working wavelength of 1550 nm has been investigated by using the finite element method (FEM). We select a typical holey fiber in which the cross section of the cladding is a solid core surrounded by a circular air holes of a three-layer regular hexagon array. In order to improve the birefringence of the structure, we replaced the six circular air holes around the core with elliptical air holes. This improved structure allows the x-polarized mode and y-polarized mode to achieve a more distinct separation at the resonant wavelength. In addition, we analyzed the effect of the elliptical hole arrangement, the ellipticity of the ellipse, the thickness of the gold-coated film, the size of the gold-coated holes and the numbers of gold-coated holes on the performance of the polarization filter. Furthermore, our designed polarization filter has excellent characteristics at the wavelength of 1550 nm. The PCF structure designed in this paper can be applied to the production of polarizing filters with compact and wide bandwidth.

2. Structure Design and Improvement

2.1 Initial Structure of the PCF and Numerical Analysis

The first PCF was successfully prepared in the laboratory by Knight et al [1] , which was a solid core surrounded by a cylindrical hole in a regular hexagonal array. With the development of technology, the fabrication process of PCFs has been greatly improved. The PCFs with simple structure can be fabricated and applied in many different fields. The easiest PCFs are those that employ index guiding as is shown in Fig. 1(a). They guide light by virtue of the smaller average refractive index of the cladding relative to the core. So we choose this type of the PCFs as the initial research object. Compare with the prior arts, the similarity is that the cross section of the cladding is a regular triangular lattice of circular air holes within the uniform dielectric medium. For the sake of enhancing the asymmetry of the structure, we deliberately enlarge the diameter of the outermost air holes and select two gold coating layers in the y direction,

Based on the structure of Fig. 1(a), we make some improvement. The cladding of the structure is composed of three layers of regular hexagonal circular air holes. For the sake of enhancing the asymmetry of the structure, we make the diameters of the outermost air holes to be larger than other layers of air holes. The diameters of outermost air holes and the rest air holes are $d2 = 2.4$ um and $d1 = 1.6$ um, respectively. The pitch of the adjacent air holes is $\Lambda = 2.8$ um. Two holes in the polarization direction can produce birefringence, which allows one of the polarization directions more sensitive, so we select the gold coating layers in the y direction. Therefore, the schematic diagram of the cross-sectional structure of the designed original gold-coated PCF is shown in Fig. 1(b).

The red sections of the two air holes are coated with gold, on which the surface plasmon polaritons (SPP) mode can form. The diameters of the gold-coated holes are $dm = 1.6$ um with the thickness of $t_{gold} = 50$ nm. The matrix material is pure silica. Since the holes reduce the refractive index of the
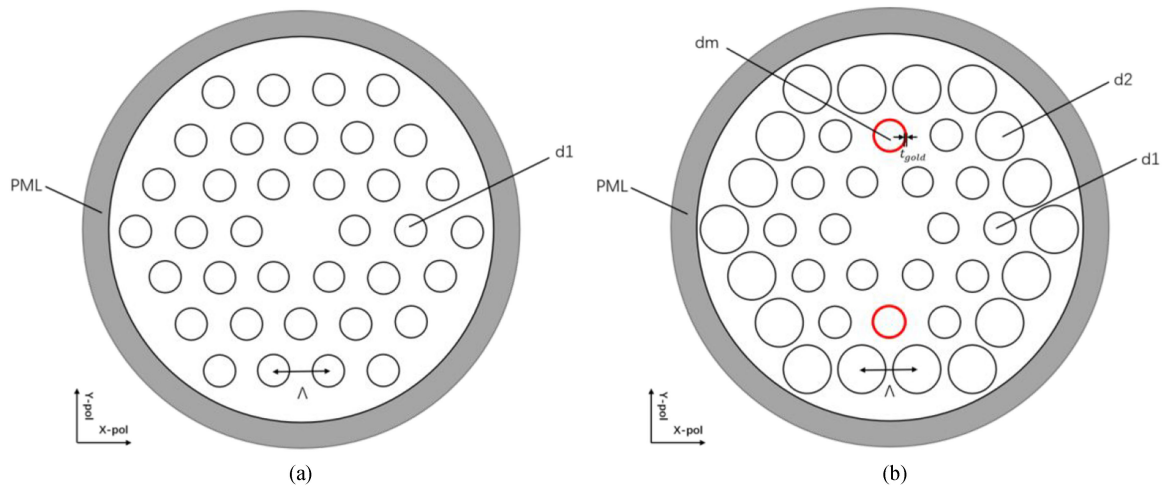
Fig. 1. Cross-section of the PCF. (a) Holey fiber that confines light in a solid core by index guiding. (b) The designed initial cross-section view of the PCF.

pure silica, the phase matching condition between the fundamental mode and the plasma mode can be ensured.

As for the complex variability of PCF structure, the FEM can usually get more accurate calculation. We use COMSOL software for numerical analysis. A perfectly matched layer (PML) is used to absorb boundary reflection waves of various angles and achieve better phase matching conditions. In order to make the numerical analysis more accurate, we take the material dispersion of the matrix material and coating material into consideration. The material dispersion coefficient of pure silica can be expressed by Sellmeier equation [20]:

$$n^2(\lambda) = 1 + \frac{B_1\lambda^2}{\lambda^2 - C_1} + \frac{B_2\lambda^2}{\lambda^2 - C_2} + \frac{B_3\lambda^2}{\lambda^2 - C_3}, \tag{1}$$

Where n is the wavelength-dependent refractive index of pure silica, and λ is the input wavelength. B1, B2, B3, C1, C2, and C3 are the Sellmeier constants.

The material dispersion coefficient of gold can be expressed by the Drude-Lorentz model [21]:

$$\varepsilon_m = \varepsilon_\infty - \frac{\omega_D^2}{\omega(\omega + j\gamma_D)} - \frac{\Delta\varepsilon\Omega_L^2}{(\omega^2 - \Omega_L^2) + j\Gamma_L\omega} \tag{2}$$

Where $\varepsilon_m\varepsilon_\infty$ is the relative high-frequency permittivity, $\Delta\varepsilon$ can be interpreted as a weighting factor, ω is the angular frequency of the incident light, ω_D and γ_D are the plasma and damping frequencies, Ω_L and Γ_L represent the frequency and the spectral width of the Lorentz oscillator. Here $\varepsilon_\infty = 5.9673$, $\Delta\varepsilon = 1.09$, $\omega_D/2\pi = 2113$, $\gamma_D/2\pi = 15.92$, $\Omega_L/2\pi = 650.07$, $\Gamma_L/2\pi = 104.86$.

The mode confinement loss is one of the most important parameters of a filter and can be calculated as [22]:

$$L(x, y) = \frac{40\pi}{\lambda \ln 10} \text{Im}(n_{eff}) \times 10^4 = 8.686 \times \frac{2\pi}{\lambda} \text{Im}(n_{eff}) \times 10^4 \text{dB/cm}, \tag{3}$$

Where $\text{Im}(n_{eff})$ is the imaginary part of the effective refractive index.

In this paper, when the phase of the core mode matches the surface plasmon, the PCF core beam is strongly coupled to the surface plasma of the gold film. The core guide mode has a loss peak. The peak of the loss is the resonance intensity. In Fig. 2, there are two resonance peaks, x-pol and y-pol, respectively. The two resonance intensities are basically the same but the resonance intensity in the y-polarized direction at the communication band $\lambda = 1.31$ um is only 30.14 dB/cm. Data show that the resonance intensity is too weak, which is not suitable for polarization filtering. Meanwhile, the resonance intensity at $\lambda = 1.55$ um in the x-pol direction is 23.26 dB/cm and in the
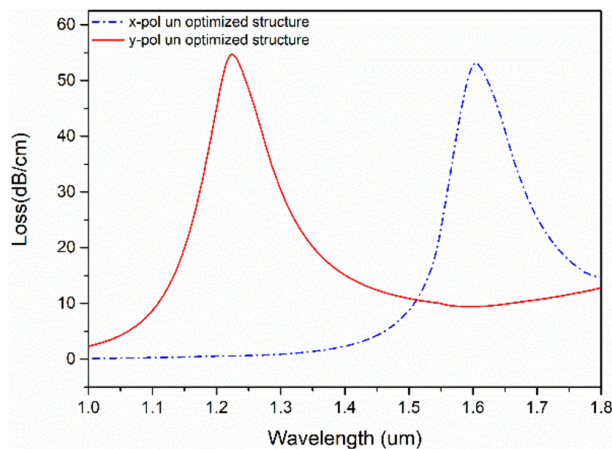
Fig. 2. The loss spectra of core mode of the unimproved structure.
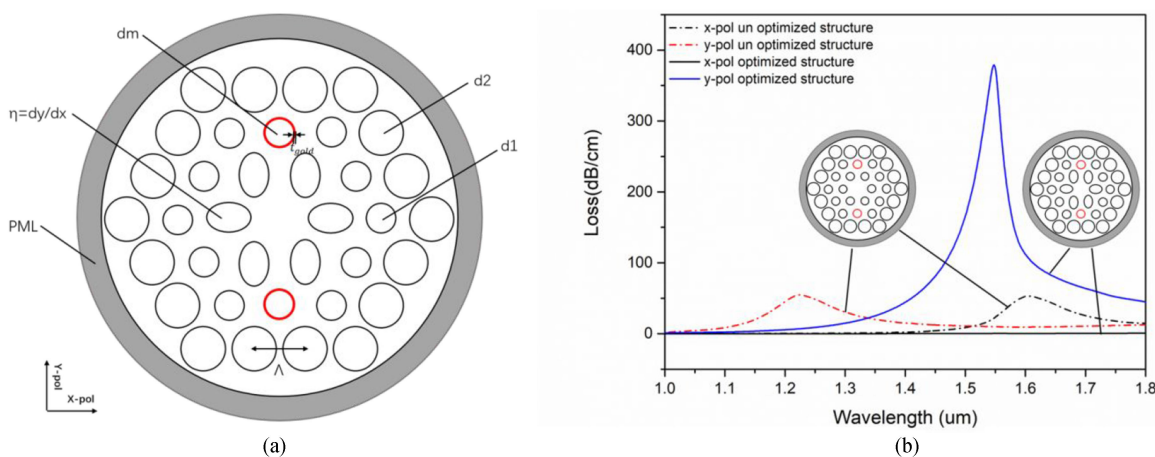
Fig. 3. (a) The improved structure of the PCF. (b) The loss spectra comparison chart of core mode of the improved and original PCF.

y-pol direction is 10.02 dB/cm. Although x polarization and y polarization can be clearly separated, it cannot work in the communication bands. Therefore, this structure requires further improvement. We decided to improve the structure by transforming the innermost six circular air holes into six elliptical air holes and find out the best elliptical hole arrangement through simulation.

2.2 Improvement Process

In this section, we deliberately introduce six elliptical holes around the core to destroy this symmetry and obtain a significant polarization effect. Fig. 3(a) is a structural diagram of our improvement. The long axis length is dy, the short axis length is dx and the corresponding ellipticity $\eta = $ dy/dx.

Fig. 3(b) is a comparison of the loss curve before and after improvement. From the Fig. 3(b), we can see clearly from the improved structure that the resonance intensity of the y-polarized direction is much larger than the x-polarized direction due to the highly asymmetrical structure of the ellipse. In the meantime, y polarization direction formant is blue-shifted. We observed that the confinement loss is 442 dB/cm at the communication wavelength of 1550 nm while the loss of x direction is only 0.0316 dB/cm. So the characteristics of filter are obvious. The following section will discuss the performance of the polarization filter based on this structure.

The characteristics of PCF polarization filter are determined by multi-variable parameters. The arrangement of elliptical holes, the ellipticity (η) of the ellipse, the thickness of the gold-coated film,
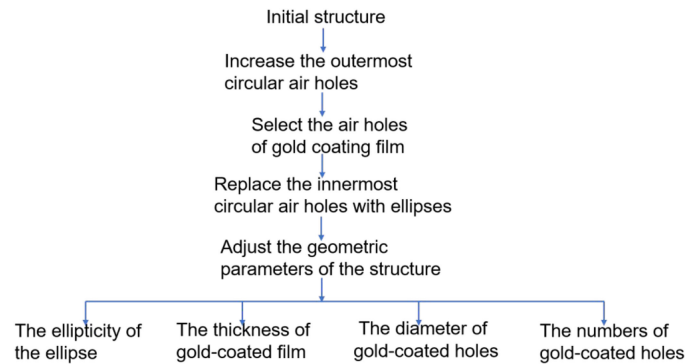
Fig. 4. The flow-chart figure of the process of improvement.
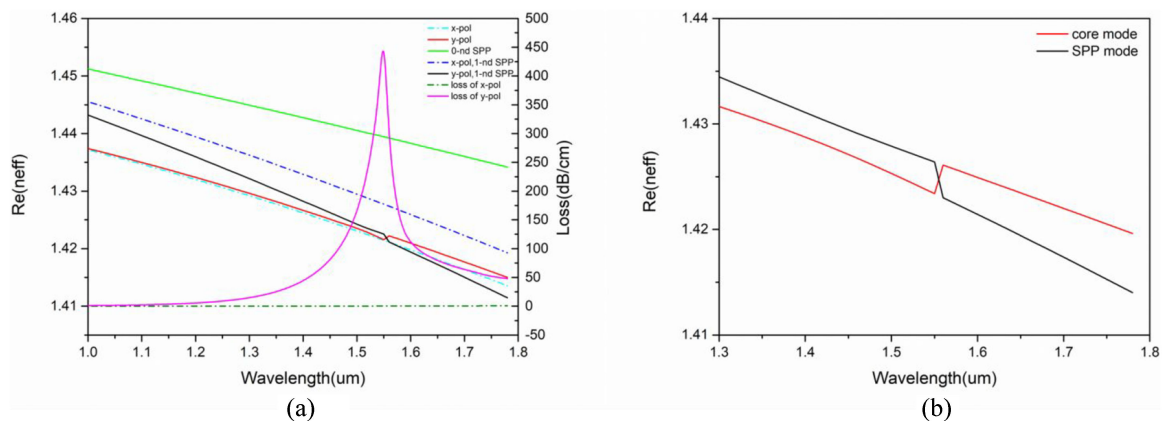
Fig. 5. (a) Dispersion relation of the core-guided mode (red solid line), SPP mode (black solid line), and loss spectrum (pink solid line). The resonance wavelength of the Y-polarization direction is 1.55 um. (b) A Real part of first-order SPP mode and y-polarized mode effective index.

the diameter of the gold-coated holes (dm) and the numbers of gold-coated holes are important parameters that have effects on the performance of the polarization filter. Based on the designed original gold-coated PCF, we improved this structure, in which the diameters of the circular air holes are d1 and d2, respectively and the pitch of the adjacent air holes (Λ) are constant. First, we change the innermost six circular air holes to elliptical and find the best arrangement of elliptical holes. Second, the effects of the ellipticity of the elliptical holes on the performance of filter is discussed. We fix dm and the thickness of the gold-coated film and the optimal ellipticity is obtained by changing the dx and dy of the ellipse. Third, dm is fixed and the improved ellipticity is substituted. The influence factor of the thickness of the gold-coated film is analyzed. At last, we change dm to obtain optimal gold-coated hole diameter and the number of gold-coated holes is considered.

In order to present the whole process of improvement, we add a flow-chart figure as is shown in Fig. 4.

2.3 Dispersion Relations

Fig. 5(a) depicts the real part of the effective refractive index (RI) of the core guided mode, the effective RI of the various orders of the SPP mode, and the confinement loss. The effective RI of the fundamental mode of the SPP mode is much larger than the core mode, so it cannot be coupled to the core mode. However, we find that the first-order SPP mode and the core mode are completely coupled. In this study, we choose the first-order mode of SPP as the research object. On account of the high birefringence of the structure and the selective coating of holes in the y direction, plasmon resonance is easily obtained. The confinement loss at y-polarized mode results
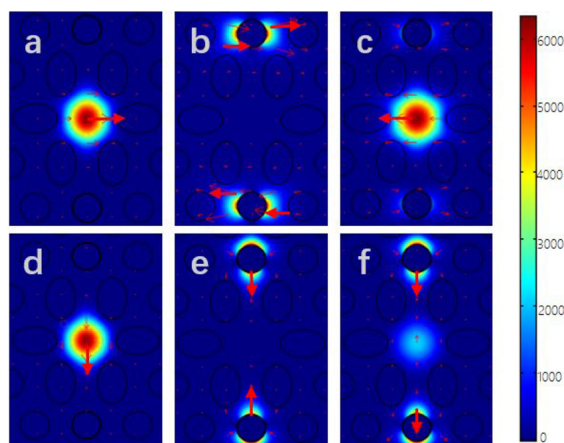
Fig. 6. Electric field distribution at the (a) x polarization direction core mode. (b) the first-order SPP mode in x polarization direction. (c) phase-matching condition in x-polarization direction. (d) y polarization direction core mode. (e) the first-order SPP mode in y polarization direction. (f) phase-matching condition in y-polarization direction.

from higher SPR interaction. The loss of x-polarized mode shows that it is inclined upwards without loss peak. The reason is that the energy of the core guided mode of the x-direction is not totally coupled into plasmon. Fully coupling occurs in the y-polarization direction, which results in a loss spike. In practice, this phenomenon can be further explained by saltation of the effective RI. Fig. 5(b) is a partial enlarged view of Fig. 5(a). It can be seen that the RI curve of the y-polarized core guided mode is abrupt at the communication wavelength of 1550 nm, at which point the core mode is coupled into the SPP mode. By this time, the energy of the core is transferred to the plasma so that the peak loss in the y direction appears at the intersection. This is a better proof of the principle that the PCF structure we designed can be applied to the polarization filter of the communication band.

Figure 6 shows the electric field distribution at $\lambda = 1550$ nm. It can be explained that the incident light enters the optical fiber (Fig. 6(a) and Fig. 6(d)) and a full emission phenomenon occurs to form an evanescent wave, which elicits a plasma wave on the gold surface, as showed in Fig. 6(b) and Fig. 6(e). In a specific case, the PCF core mode at a certain wavelength is consistent with the transmission constant of the surface plasmon wave of the first-order mode (in this paper the certain wavelength is 1550 nm). At this point, the light intensity in the core guided mode is greatly reduced and most of the incident light energy is absorbed by the plasmon of the gold surface. The coupling effect occurs between the two modes. In Fig. 6(f) the energy of the core guided mode of y direction is totally coupled into the plasmon while in Fig. 6(c) there is no complete resonance occurs in x direction.

3. Results and Analysis

The main properties of the polarization filter include the resonance wavelength, the resonance peak and the extinction ratio (ER). The characteristics of fiber polarization filters are determined by the geometries of PCF. These parameters should be chosen to ensure that the interaction between the evanescent wave and the metal surface plasma wave can be achieved. We discuss the effects of the arrangement of elliptical holes, the ellipticity (η) of the ellipse, the thickness of the gold-coated film, the size of the gold-coated holes and the numbers of gold-coated holes in detail on the properties of polarization filters.

3.1 Different Arrangement of Elliptical Holes With Different Losses

First we discuss the effect of the arrangement of elliptical holes on the properties of the polarization filter. The four arrangement modes are as follows as shown in Fig. 7: all elliptical holes are arranged
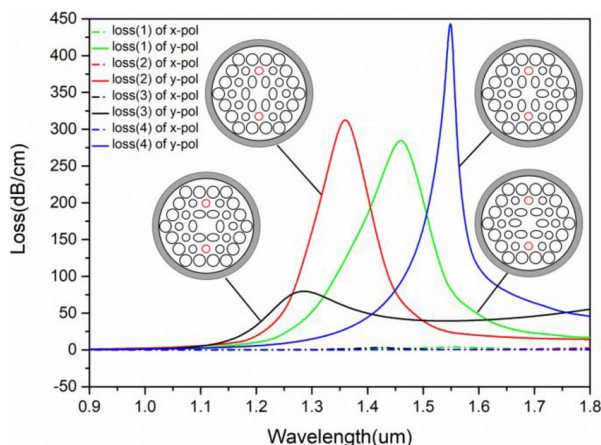
Fig. 7. Confinement loss for different arrangement of elliptical holes with x direction (dashed) and y direction (solid).

horizontally (green curve) , all elliptical holes are arranged vertically (red curve), upper and lower placed horizontal elliptical holes while left and right sides placed vertical elliptical holes (black curve), upper and lower placed vertically elliptical holes while left and right sides placed horizontal elliptical holes (blue curve). The core mode loss spectra corresponding to these four arrangements are shown in Fig. 7. The losses of x polarization direction are very low, almost zero, which is beneficial to achieve polarization filtering. From the perspective of the resonance peak, it can be observed that the upper and lower elliptical holes are in vertical arrangement are much larger than they are in horizontal arrangement. Therefore, the red curve and the blue curve are preferred. From the point of view of resonance wavelength, we expect that the polarization filter can work in the 1550 nm communication band because our designed PCF has the least loss of light intensity when transmitting in this window. We found the blue curve has a resonance peak at a wavelength equal to 1358 nm. Based on the above two factors, we choose the elliptical hole distribution pattern in line corresponding to the blue curve, that is, the upper and lower elliptical holes are arranged vertically and the left and right elliptical holes are horizontally arranged as the optimal structure.

3.2 Different Ellipticities of Elliptical Holes With Different Losses

This section will discuss the effects of the η of elliptical holes on filter performance. As we know, the η of the elliptical hole around the core not only affects the birefringence of the structure but also the distribution of light transmission energy. Therefore, in order to achieve good polarization characteristics and obtain efficient transmission quality, it is necessary to have an improved size of ellipse.

We set d1 = 1.6 um, d2 = 2.4 um, dm = 1.5 um, respectively. The thickness of gold-coated film is 50 nm, the lattice constant is Λ = 2.8 um. In order to change the ellipticity, we fixed the ellipse parameter dy = 1.2 um and only change dx from 0.4 um to 0.8 um at an interval of 0.2 corresponding to η of 3 to 1.5 as shown in Fig. 8(a). Then we keep the ellipse parameter dx = 0.4 um as a constant, and dy is varied from 0.6 um to 1.2 um as shown in Fig. 8(b). Comparing the two figures at the same ellipticity, the resonance wavelength of the Fig. 8(b) is shifted to the short wavelength direction, and the resonance peak is also slightly lowered. As the η increases, on the one hand, the resonant wavelength shifts blue and the plasmon resonance strength decreases. On the other hand, the increase of η leads to moderate increase in the loss of the x-polarization direction. According to the graph, the loss in x direction increases to 18.16 dB/cm as η is up to 3. It can be understood that the increase in η promotes the permeation of light from the cladding, thereby weakening the resonance intensity. So dx = 0.8 um is the best value and the corresponding ellipticity is 1.5.
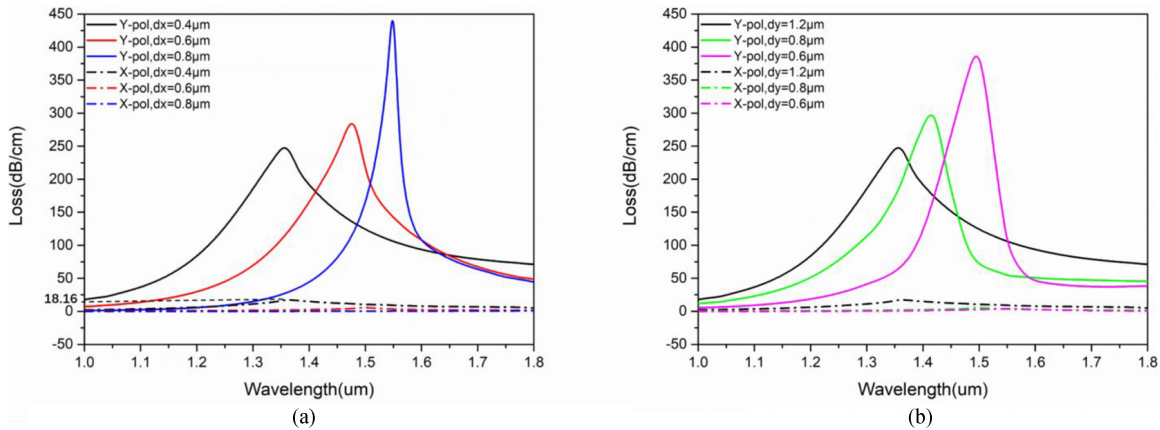
Fig. 8. Confinement loss for different ellipticities of elliptical holes with x direction (dashed) and y direction (solid). (a) fix dy and change dx from 0.4 um to 0.8 um. (b) fix dx and change dy from 0.6 um to 1.2um.
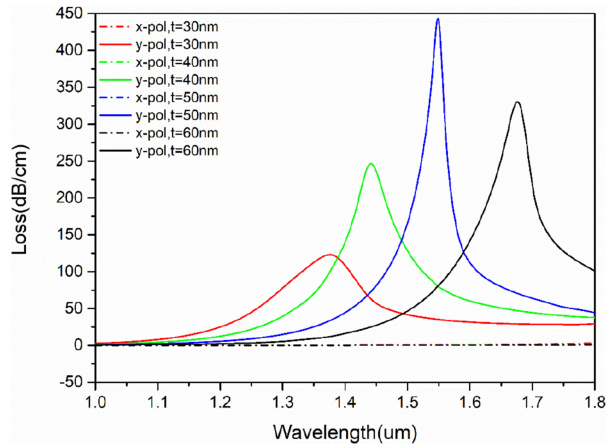
Fig. 9. Confinement loss for different thickness of the gold layer with x direction (dashed) and y direction (solid).

3.3 Different Thickness of the Gold Film With Different Losses

In the section, we compare the effects of different gold-coated film thicknesses on the filter performance. we set the cladding air hole diameters $d1 = 1.6$ um, $d2 = 2.4$ um, $dm = 1.6$ um, respectively. The elliptical hole parameter $dy = 1.2$ um, $dx = 0.8$ um. The lattice constant $\Lambda = 2.8$ um. The thickness of gold coating film varies from 30 nm to 60 nm with an interval of 10 nm.

It is easy to find from Fig. 9 that the plasma wave on the metal surface is very sensitive to the thickness variation of the metal film. As the thickness of the gold coating film increases, the resonance peak firstly undergoes a process of increasing and then decreasing while the resonance wavelength is always red-shifted. This phenomenon is consistent with the paper [23], [24]. Therefore, it is inferred that the degree of coupling depends on the thickness of the gold coating film. Each wavelength corresponds to an optimal metal film thickness. We can further explain this phenomenon following as when the gold coating is thick, for example 60 nm, the electric field is difficult to penetrate the metal which results in significant suppression of the loss depth. A thinner gold layer results in a weaker coupling between the fundamental mode and the plasma mode. So it is necessary to select the appropriate metal thickness. From the curve trend, the required polarization characteristics can be obtained at $t_{gold} = 50$ nm.
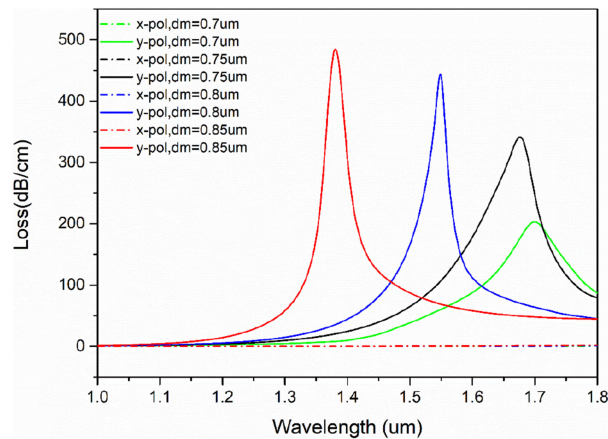
Fig. 10. Confinement loss for different gold plated hole diameters with x direction (dashed) and y direction (solid).

3.4 Different Gold-Coated Hole Diameters With Different Losses

Through the previous analysis, the structural parameters including small air hole diameter d1, large air hole diameter d2, the ellipticity of elliptical holes η, hole spacing Λ, gold coating film thickness t_{gold} = 50nm are basically determined. We have found that filter performance also varies with the size of the gold-coated holes. In order to investigate the effect of gold-coated hole diameters (dm) on the core guided mode loss, we set the above parameters constant, and the dm increase from 0.7 um to 0.85 um with an interval of 0.05 um.

As illustrated in Fig. 10. the loss of PCF is greatly affected by dm. With the dm increases, the loss peak increases gradually while the resonant wavelength is blue-shifted. The reason for this phenomenon is that as the diameter increases, the distance between the metal layer and the fiber core becomes closer, which enhance coupling capability. It can be seen from the Fig. 10 that by adjusting the size of the gold-coated hole, the resonance peak will change. This means that the polarization filter can be implemented in different bands. For the 1550 nm communication band, in this paper we choose dm = 0.8 um.

3.5 Different Numbers of the Gold-Coated Holes With Different Losses

Based on the above, it can be concluded that changing the geometric parameters of the PCF can improve the performance of the polarization filter. The effect of the location and number of gold-coated holes will be examined in this section. At the same time, the gold-coated holes are filled with pure water. Water is selected as the filling material because the absorption loss of the water itself is negligible at the wavelength of 1550 nm.

In this paper, the confinement loss curves of two gold-coated holes, four gold-coated holes and six gold-coated holes are compared in Fig. 11. From the view of fabrication process, this selected six gold-coated hole structure is easier to manufacture. According to the reference [25], the structure of the selective metal coating film can be produced. The results show that after the four holes are coated with gold, although the loss in the communication band is only 242.25 dB/cm, there are two peaks of 443 db/cm and 452 db/cm, respectively. Corresponding to the wavelengths of 1.52 um and 1.60 um. When six holes are selected to be coated with the gold film, as the wavelength increases, the tendency of the loss curve becomes very complicated and the peak does not undergo significant separation. In a sum, the structure of two gold-coated holes are suitable for making a polarization filter. In addition, we have found that the addition of pure water only enhances the coupling ability without changing the position of the formant.
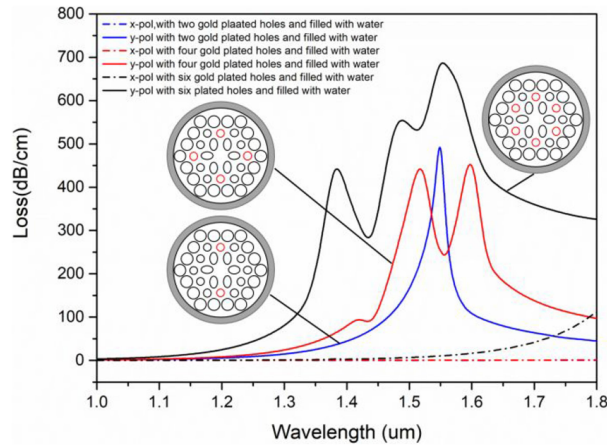
Fig. 11. Confinement loss for different positions of the gold plated hole with x direction (dashed) and y direction (solid).
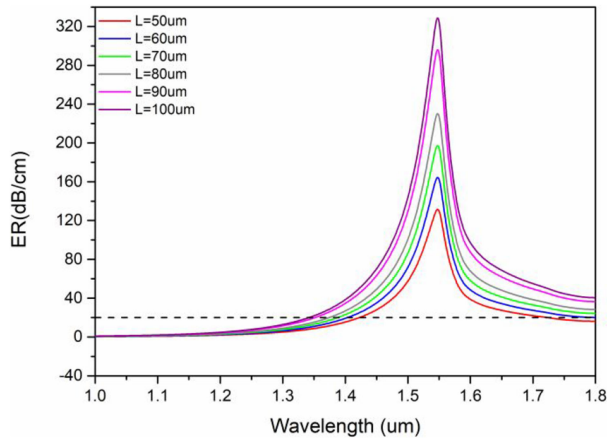
Fig. 12. The ER of improvement results for the filter with gold layer, the ER of the designed PCF when the fiber length ranges from 50 um to 100 um with the parameter of d1 = 1.6 um, d2 = 2.4 um, dm = 1.6 um, Λ = 2.8 um and t_{gold}= 50nm.

3.6 Extinction Ratio

Through the above analysis, we designed the optimal PCF polarization filter structure. The extinction ratio(ER) is an important parameter for evaluating the performance of the polarizing filter, which can characterize the transmission performance of a filter. The extinction ratio depends on the length of the fiber and can be expressed by the following formula:

$$CT = 20\lg\{\exp\left[(\alpha_1-\alpha_2)L\right]\},\qquad(4)$$

Where $\alpha1$ and $\alpha2$ represent the confinement loss of the x-polarization direction and the y-polarization direction, respectively. L is the length of the optical fiber. We set the fiber length range from 50 um to 100 um with an interval of 10 um. The dependence of ER on the wavelength of different fiber lengths are shown in Fig. 12. The available optical bandwidth is defined as the wavelength range above 20 dB or below −20 dB. As shown in Fig. 12, at L = 100 um, the ER can reach to 326 dB at a wavelength of 1550 nm. When L is 50 um, the ER is better than 20 dB and the bandwidth is 300 nm. It is very advantageous to make a broadband filter. More importantly, the length of the fiber is very short. The proposed PCF polarization filter has a broad application prospect in the field of micro-integration.

TABLE 1

Filter Performance by Fabrication Tolerance of Gold-Coated Film Thickness at 1550 nm

Wavelength (nm)	The fabrication tolerances analysis of $t_{gold} = 50nm$	Resonance Intensity of the y polarization (dB/cm)	The Resonance Wavelength of y polarization (nm)
1550	+5%	346.187	1569
	-5%	292.256	1527

TABLE 2

Filter Performance by Fabrication Tolerance of Gold-Coated Hole Diameter at 1550 nm

Wavelength (nm)	The fabrication tolerances analysis of dm	Resonance Intensity of the y polarization (dB/cm)	The Resonance Wavelength of y polarization (nm)
1550	+5%	396.589	1582
	-5%	461.136	1522

The fabrication tolerances analysis is of great importance. The thickness of the gold-coated film and the diameter of the gold-coated hole have significant influences on the performance of the designed PCF polarization filter. We discuss the effects of geometric error of gold film thickness. According to Fig. 9, the optimal gold film thickness is 50 nm. We change $\pm 5\%$ based on this value to analyze the characteristics of filter. It can be seen from table 1 that the optimum resonance peak is no longer 1550 nm. When the thickness of the gold-coated film increases by 5%, the resonance wavelength shifts to 1569 nm. The resonance intensity of the y-polarization direction is 346.187 dB/cm, which is also much larger than X polarization. The best diameter of the gold-coated hole is shown in Fig. 10. Table 2 shows the performance of the filter with the gold-coated hole diameter in the range of $\pm 5\%$, the resonance wavelength varies around 1550 nm. In this case, great separation can be achieved in the x and y direction and the PCF we proposed has good tolerance to fabrication tolerances.

4. Conclusion

We propose a gold-coated PCF polarization filter with a wide bandwidth. Based on plasmon resonance, the introduction of elliptical holes with a specific position distribution around the core results in a large confinement loss of the fundamental mode in y polarization direction. Numerical analysis shows that the designed polarization filter is sufficient, especially in the communication band of 1550 nm. The loss of y polarization direction can reach to 442 dB/cm, while the loss of x polarization direction is only 0.0316 dB/cm. In addition, the resonance peak changes with the thickness and size of the gold-coated holes, which means the filter can be applied to different wavelength bands. The number of gold-coated holes is also considered. When the length of the fiber is 1 mm, the extinction ratio comes up to 326 dB/cm. The applicable bandwidth reaches to 300 nm while the fiber length is only 50 um. It is easy to make a small broadband filter. Based on above results, we have designed a polarization filter which can be applied to integrated, high-capacity, broadband optical communication systems.

Acknowledgment

References

[1] J. C. Knight, T. A. Birks, P. St. J. Russell, and D. M. Atkin, "All-silica single-mode optical fiber with photonic crystal cladding," *Opt. Lett.*, vol. 21, no. 19, pp. 1547–1549, 1996.

[2] B. Shuai, L. Xia, Y. Zhang, and D. Liu, "A multi-core holey fiber based plasmonic sensor with large detection range and high linearity," *Opt. Exp.*, vol. 20, no. 6, pp. 5974–5986, 2012.

[3] P. S. J. Russell, "Photonic-crystal fibers," *Science*, vol. 299, no. 12, pp. 4729–4749, 2007.

[4] D. Zografopoulos and E. Kriezis, "Tunable polarization properties of hybrid-guiding liquid-crystal photonic crystal fibers," *J. Lightw. Technol.*, vol. 27, no. 6, pp. 773–779, Mar. 2009.

[5] B. Sun *et al.*, "Unique temperature dependence of selectively liquid-crystal-filled photonic crystal fibers," *IEEE Photon. Technol. Lett.*, vol. 28, no. 12, pp. 1282–1285, Jun. 2016.

[6] A. Mahmood, V. Kavungal, S. S. Ahmed, G. Farrell, and Y. Semenova, "Magnetic-field sensor based on whispering-gallery modes in a photonic crystal fiber infiltrated with magnetic fluid," *Opt. Lett.*, vol. 40, no. 21, pp. 4983–4986, 2015.

[7] J. N. Dash and R. Jha, "Graphene-based birefringent photonic crystal fiber sensor using surface plasmon resonance," *IEEE Photon. Technol. Lett.*, vol. 26, no. 11, pp. 1092–1095, Jun. 2014.

[8] H. Li, S. G. Li, H. L. Chen, J. S. Li, G. W. An, and J. C. Zi, "A polarization filter based on photonic crystal fiber with asymmetry around gold-coated holes," *Plasmonics*, vol. 11, no. 1, pp. 103–108, 2016.

[9] C. Dou, X. L. Jing, S. G. Li, Q. Liu, and J. Bian, "A photonic crystal fiber polarized filter at 155 μm based on surface plasmon resonance," *Plasmonics*, vol. 11, no. 4, pp. 1163–1168, 2016.

[10] P. K. Maharana, T. Srivastava, and R. Jha, "Ultrasensitive plasmonic imaging sensor based on graphene and silicon," *IEEE Photon. Technol. Lett.*, vol. 25, no. 2, pp. 122–125, Jan. 2013.

[11] M. R. Hasan *et al.*, "Spiral photonic crystal fiber-based dual-polarized surface plasmon resonance biosensor," *IEEE Sensors J.*, vol. 18, no. 1, pp. 133–140, Jan. 2018.

[12] Y. You, "Polarization-sensitive tunable filter in a one-dimensional photonic crystal consisting of anisotropic metamaterials with arbitrary optical axis," *Physica B*, vol. 405, no. 7, pp. 1842–1845, 2010.

[13] M. Djavid, A. Ghaffari, F. Monifi, and M. S. Abrishamian, "T-shaped channel-drop filters using photonic crystal ring resonators," *Physica E*, vol. 40, no. 10, pp. 3151–3154, 2008.

[14] J. S. Li, "Terahertz wave narrow bandpass filter based on photonic crystal," *Opt. Commun.*, vol. 283, no. 13, pp. 2647–2650, 2010.

[15] U. Fano, "The theory of anomalous diffraction gratings and of quasi-stationary waves on metallic surfaces," *J. Opt. Soc. Amer.*, vol. 31, no. 31, pp. 213–222, 1941.

[16] T. S. Wu *et al.*, "Surface plasmon resonance biosensor based on gold-coated side-polished hexagonal structure photonic crystal fiber," *Opt. Exp.*, vol. 25, no. 17, pp. 20313–20322, 2017.

[17] A. Nagasaki, K. Saitoh, and M. Kashiba, "Polarization characteristics of photonic crystal fibers selectively filled with metal wires into cladding air holes," *Opt. Exp.*, vol. 19, no. 4, pp. 3799–3808, 2011.

[18] A. Khaleque and H. T. Hattori, "Ultra-broadband and compact polarization splitter based on gold filled dual-core photonic crystal fiber," *J. Appl. Phys.*, vol. 118, no. 14, pp. 682–683, 2015.

[19] L. H. Jiang, Y. Zheng, J. Yang, L. T. Hou, Z. H. Li, and X. T. Zhao, "An ultra-broadband single polarization filter based on plasmonic photonic crystal fiber with a liquid crystal core," *Plasmonics*, vol. 12, no. 2, pp. 411–417, 2017.

[20] L. Peng, F. K. Shi, G. Y. Zhou, S. Ge, Z. Y. Hou, and C. M. Xia, "A surface plasmon biosensor based on a D-shaped microstructured optical fiber with rectangular lattice," *IEEE Photon. J.*, vol. 7, no. 5, Oct. 2015, Art. no. 4801309.

[21] A. Vial, A. Grimault, D. Macłas, D. Barchiesi, and M. Chapelle, "Improved analytical fit of gold dispersion: Application to the modeling of extinction spectra with a finite-difference time-domain method," *Phys. Rev. B*, vol. 71, no. 8, 2005, Art. no. 85416.

[22] K. Saitoh, M. Koshiba, T. Hasegawa, and E. Sasaoka, "Chromatic dispersion control in photonic crystal fibers: Application to ultra-flattened dispersion," *Opt. Exp.*, vol. 11, no. 8, pp. 843–852, 2003.

[23] A. A. Rifat, R. Ahmed, G. A. Mahdiraji, and F. R. M. Adikan, "Highly sensitive D-shaped photonic crystal fiber-based plasmonic biosensor in visible to near-IR," *IEEE Sensors J.*, vol. 17, no. 9, pp. 2776–2783, May 2017.

[24] H. K. Qu *et al.*, "Two-core single-polarization optical fiber with a large hollow coated bimetallic layer," *Appl. Opt.*, vol. 57, no. 10, pp. 2446–2451, 2018.

[25] D. J. J. Hu and H. P. Ho, "Recent advances in plasmonic photonic crystal fibers: Design, fabrication and applications," *Adv. Opt. Photon.*, vol. 9, no. 2, pp. 257–314, 2017.